A new method of terrain correcting airborne gravity gradiometry data using 3D Cauchy-type integrals

Michael S. Zhdanov, University of Utah and TechnoImaging, Glenn A. Wilson, TechnoImaging, and Xiaojun Liu, University of Utah*

Summary

We introduce 3D Cauchy-type integrals that extend the classic theory of Cauchy integrals to 3D potential fields. In particular, we show how we are able to evaluate the gravity and gravity gradiometry responses of 3D bodies as surface integrals over arbitrary volumes that may have spatially variable densities. This entirely new method of 3D spatial-domain modeling is particularly suited to the terrain correction of airborne gravity gradiometry (AGG) data. The surface integrals are evaluated numerically on a topographically conforming grid with a resolution equal to the digital elevation model (DEM). Thus, our method directly avoids issues related to prismatic discretization of the digital elevation model, and their associated volume integration. We demonstrate this with a model study for AGG data simulated for a 1 Eö/√Hz system over the Kauring test site in Western Australia.

Introduction

Zhdanov (1984, 1988) introduced the theory of Cauchy-type integrals for 3D potential fields. Unfortunately, this interesting and fundamental area of potential field theory has since been dormant. In this paper, we revive the study of 3D Cauchy-type integrals for potential fields. In particular, we have developed an entirely new method for the 3D modeling of gravity fields and their gradients as surface integrals over arbitrary volumes that may have spatially variable densities. An obvious application of this modeling is for improved terrain correction of airborne gravity gradiometry (AGG) data, which is a means of reducing the dynamic range of AGG data so as to reveal the more subtle geological responses present. A number of factors influences the validity of terrain corrections, and these include the accuracy of the aircraft position, resolution of the DEM, the way the terrain is approximated, and the methods used to filter the predicted responses to match the AGG's acquisition system and post-acquisition processing (e.g., Kass and Li, 2008; Dransfield and Zeng, 2009; Davis et al., 2011). These factors are particularly important for terrain corrections to sub-Eö levels, particularly as the next generation of 1 Eö/√Hz AGG systems are now being developed and tested. By using 3D Cauchy-type integrals, we can evaluate the terrain response as a surface integral over the DEM. This surface integration ensures accurate representation of the terrain response. Moreover, the method directly avoids issues related to prismatic discretization of the digital elevation model, and their associated volume integration problems.

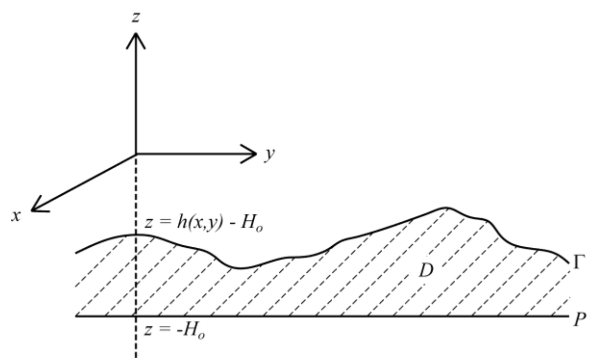

Figure 1. *Schematic of the 3D terrain model, D, contained within a surface, Γ, described by any arbitrary function h(x,y), and a lower plane P. The density distribution within the terrain may be spatially variable.*

3D Cauchy-type integrals and their properties

The concept of a 3D Cauchy-type integral for potential fields was introduced by Zhdanov (1984, 1988), and is represented by the following expression:

$$\mathbf{C}^S(\mathbf{r},\boldsymbol{\varphi}) = -\frac{1}{4\pi}\iint_S \left[(\mathbf{n}\cdot\varphi)\nabla\frac{1}{|\mathbf{r}-\mathbf{r}'|} + (\mathbf{n}\times\varphi)\times\nabla\frac{1}{|\mathbf{r}-\mathbf{r}'|}\right]ds, \quad (1)$$

where S is come closed surface, $\boldsymbol{\varphi} = \boldsymbol{\varphi}(\mathbf{r})$ is some vector function specified on S and continuous on S, and $\mathbf{n}$ is a unit vector of the normal to S directed outside the domain D, bounded by the surface S. Function $\boldsymbol{\varphi}$ is called a vector density of the Cauchy-type integral $\mathbf{C}^S(\mathbf{r},\varphi)$. It has been shown that everywhere outside S, the vector function $\mathbf{C}^S$ satisfies to the following equations:

$$\nabla'\cdot\mathbf{C}^S(\mathbf{r}',\boldsymbol{\varphi}) = 0,\ \ \nabla'\times\mathbf{C}^S(\mathbf{r}',\boldsymbol{\varphi}) = 0, \quad (2)$$

where prime denotes a differentiation over vector variable $\mathbf{r}'$. Therefore, vector field $\mathbf{C}^S(\mathbf{r},\varphi)$ is Laplacian and its scalar components are harmonic functions everywhere outside the surface S. In the special case where $\boldsymbol{\varphi}(\mathbf{r})$ represents the boundary values on S of the gradient of a function harmonic inside domain D, we have the following Cauchy integral formula:

© 2012 SEG

$$\mathbf{C}^S(\mathbf{r}',\boldsymbol{\varphi}) = \begin{cases}\boldsymbol{\varphi}(\mathbf{r}'), & \mathbf{r}' \in D,\\ 0, & \mathbf{r}' \in CD,\end{cases} \quad (3)$$

where *CD* is an infinite domain complementing the closed domain, $\bar{D} = D + S$, with respect to the whole space. The remarkable property of the 3D Cauchy-type integral is that in the 2D case, equation (1) is reduced to the classical Cauchy integral of the theory of the functions of complex variable. One important formula from the classical theory of the functions of complex variables is the Pompei formula, which solves the boundary value problem for arbitrary function of the complex variable. Following Zhdanov (1984, 1988) and Davies et al. (1989), one can formulate a 3D analog of Pompei formula for a potential field, $\mathbf{F}$, defined within a domain, D:

$$\mathbf{C}^S(\mathbf{r}',\mathbf{F}) + \frac{1}{4\pi}\iiint_D (\nabla\cdot\mathbf{F})\nabla\frac{1}{|\mathbf{r}-\mathbf{r}'|}dv = \begin{cases}\mathbf{F}(\mathbf{r}'), & \mathbf{r}' \in D,\\ 0, & \mathbf{r}' \in CD,\end{cases} \quad (4)$$

where the vector field satisfies the equations: $\nabla\times\mathbf{F} = 0$, $\mathbf{r}\in D$. The derivation of the Pompei formula (4) is based on the Gauss theorem, and provides a solution of the boundary-value problem for an arbitrary potential field.

Representing the gravity field and its gradients in terms of 3D Cauchy-type integrals

The gravity field satisfies the following equations:

$$\nabla\cdot\mathbf{g} = -4\pi\gamma\rho_0\mathbf{r}, \qquad \nabla\times\mathbf{g} = 0, \quad (5)$$

where γ is the universal gravitational constant, and ρ_0 is a constant density of a 3D volume of masses within some domain, D. We assume that the vector field, $\mathbf{F}$, has the form:

$$\mathbf{F} = -\frac{4\pi}{3}\gamma\rho_0\mathbf{r}, \text{ and } \nabla\cdot\mathbf{F} = 4\pi\gamma\rho_0, \quad (6)$$

Substituting equations (6) into the 3D Pompei formula (4):

$$\mathbf{C}^S\left(\mathbf{r}',\frac{4\pi}{3}\gamma\rho_0\mathbf{r}\right) + \gamma\iiint_D \rho_0\nabla\frac{1}{|\mathbf{r}-\mathbf{r}'|}dv = \begin{cases}\frac{4\pi}{3}\gamma\rho_0\mathbf{r}', & \mathbf{r}' \in D,\\ 0, \mathbf{r}' \in CD,\end{cases} \quad (7)$$

The volume integral in the left-hand part of equation (7) is (with the negative sign) the gravity field of a domain, D:

$$\mathbf{g}(\mathbf{r}') = -\gamma\iiint_D \rho_0\nabla\frac{1}{|\mathbf{r}-\mathbf{r}'|}dv, \quad (8)$$

expressed in the well-known form of a volume integral. At the same time, it is useful to express the same gravity field in terms of a surface integral over the domain, D.

Thus, we arrive at a representation of the gravity field in terms of a 3D Cauchy-type integral:

$$\mathbf{g}(\mathbf{r}') = \begin{cases}-\frac{4\pi}{3}\gamma\rho_0\mathbf{r}' + \frac{4\pi}{3}\gamma\rho_0\mathbf{C}^S(\mathbf{r}',\mathbf{r}), & \mathbf{r}' \in D,\\ \frac{4\pi}{3}\gamma\rho_0\mathbf{C}^S(\mathbf{r}',\mathbf{r}), & \mathbf{r}' \in CD.\end{cases} \quad (9)$$

In a case where $\mathbf{r}' \in CD$, we have:

$$\mathbf{g}(\mathbf{r}') = \frac{4\pi}{3}\gamma\rho_0\mathbf{C}^S(\mathbf{r}',\mathbf{r}). \quad (10)$$

Similar expressions can be derived for the tensor of gravity gradient, $\mathbf{G}$:.

$$\mathbf{G}(\mathbf{r}') = \nabla'\mathbf{g}(\mathbf{r}') = \frac{4\pi}{3}\gamma\rho_0\nabla'\mathbf{C}^S(\mathbf{r}',\mathbf{r}), \quad (11)$$

where gradient of vector is represented by a dyadic product of the del operator and the corresponding vector. In the above, we have assumed that the density inside the domain D is constant. However, as discussed by Zhdanov (1988), the density of the domain can be any arbitrary continuous function, $\rho(\mathbf{r})$. This means we are able to modify the above (and following) equations to incorporate any of the analytic density-depth functions in use for describing sedimentary basins, such as linear, quadratic, parabolic, exponential, hyperbolic and polynomial functions.

Cauchy-type representation of gravity gradients for terrain with uniform density

As illustrated in Figure 1, we can consider a model of a domain D that is infinitely extended in the horizontal directions, and bound by an upper surface Γ that describes the DEM as $z = h(x,y) - H_0$, and bound by a horizontal plane $z = h_0$, where $H_0 \geq h(x,y) \geq 0$ and:

$$h(x,y) - H_1 \to 0 \text{ for } \sqrt{x^2+y^2\to\infty}, \quad (12)$$

where H_1 is a constant. The gravity field, $\mathbf{g}$, of the model can be represented by the Cauchy-type integral:

$$\mathbf{g}(\mathbf{r}') = 4\pi\gamma\rho_0\mathbf{C}^\Gamma(\mathbf{r}',(z+H_0)\mathbf{d}_z). \quad (13)$$

Similar expressions can be derived for the tensor of gravity gradient:

$$\mathbf{G}(\mathbf{r}') = \nabla'\mathbf{g}(\mathbf{r}') = 4\pi\gamma\rho_0\nabla'\mathbf{C}^\Gamma(\mathbf{r}',(z+H_0)\mathbf{d}_z). \quad (14)$$

We can discretize the Cauchy-type integrals for the gravity field and its gradients by dividing the integration plane into a rectangular mesh Σ, where each cell is divided into two triangles which form the elementary cells (Figure 2).

DOI http://dx.doi.org/10.1190/segam2012-0744.1

The significance of this method is that we can model the gravity and gravity gradient responses of any 3D domain with the geometric resolution and accuracy of its DEM. Moreover, the 3D modeling of the domain is expressed as a surface integral which may be rapidly and accurately evaluated. It is important to emphasize that, the prisms with triangulated tops (Figure 2) provides much more accurate representation of the shape of the terrain surface than a combination of the rectangular prisms used by the conventional terrain correction methods. Note also that, the standard practice of increasing discretization as a function of distance from the observation point can be easily incorporated into the surface integration.

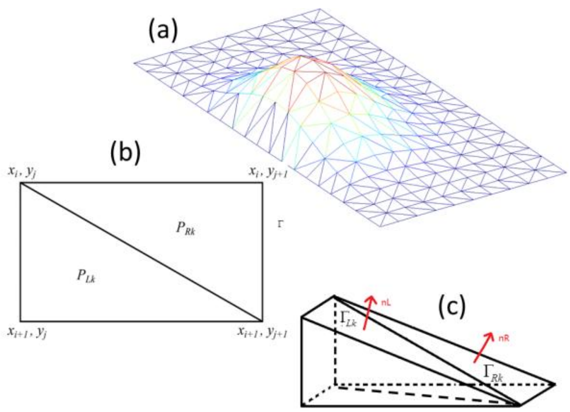

Figure 2. *Triangular discretization of the density contrast surface: (a) schematic view of triangular mesh grid; (b) each rectangular cell of the mesh* Σ *is divided into two triangles, which form the elementary cells* P_{Lk} *(left triangular) and* P_{Rk} *(right triangular); (c) 3D view of two neighbored prisms with triangulated tops,* Γ_{Lk} *and* Γ_{Rk}.

Case study – Kauring

With funding from the Western Australian government's 2009 Exploration Initiative Scheme and a matching contribution from Rio Tinto Exploration (RTX), the Geological Survey of Western Australia (GSWA) and Geoscience Australia (GA) have established the Kauring test site for testing and calibrating airborne gravity and gravity gradiometry systems (Howard et al., 2010). The site is approximately 100 km east of Perth in Western Australia, is free of low level flight restrictions, has minimal human infrastructure, and hosts gentle rolling topography of granitic terrain. The test site allows interested individuals or organizations to compare airborne data to detailed ground gravity data, or products derived from these data. It will also allow for the direct comparison of different airborne gravity and gravity gradiometry systems over the same gravity features where all other variables, besides the measuring system are defined and constant. Digital elevation models have been released for 10 m LiDAR, and 80 m SRTM.

To facilitate a comparison of 3D inversion methods during 2011, RTX developed a synthetic airborne gravity gradiometry dataset of 4687 stations (Grujic, 2012). The 3D density model contained a variety of relevant geological targets representative of discrete tunnels, nickel sulfide deposits, intrusive dikes, and kimberlites, embedded in a uniform 2.67 g/cm^3 terrain so that the wavelength, magnitude and symmetry of the data were varied. The data were simulated along a realistic drape with a mean terrain clearance of 80 m over the Kauring test site. Noise representative of a 1 Eö/√Hz (at 1 Hz) instrument was then added to the simulated free-air gravity gradiometry data. The data for the bodies were simulated by RTX using the commercial software package, *ModelVision*. Terrain response was simulated by RTX using concentric square zones around each observation. The cell size of the terrain information quadrupled for each consecutive zone, starting with a square of 800 m side length and 10 m cell size in the innermost zone. The size of the zones doubled for each consecutive zone. For example, the second zone around each station was a 1600 m wide square with a 40 m cell size. Six zones that follow this pattern were created around each observation. The grids were used to triangularly facet the terrain into vertical prisms with a uniform density of 2.67 g/cm^3 that extend to a zero level datum. Outside the available terrain information, an infinite slab with a height equal to the mean terrain elevation was modeled and added to the responses of the prisms.

In the limited space of this expanded abstract, we only show the G_{zz} responses. Figure 3 shows the simulated free-air G_{zz} response due to the bodies contaminated with 1 Eö/√Hz (at 1 Hz) noise. We terrain corrected the free-air G_{zz} data for a 2.67 g/cm^3 terrain density using a 10 m cell discretization of the merged LiDAR and SRTM digital elevation models to a square of 10 km side length centered about each station (Figure 4). This resulted in the DEM being approximated by approximately two million topographically conforming triangular cells. Figure 5 shows the noise-free G_{zz} response due to the bodies (as calculated with *ModelVision*) with no terrain effects. Differences between our terrain corrections and the true responses of the prisms can be attributed to noise and prism-based by which the terrain response was calculated (Figure 6). We observed averaged differences of 0.34 Eo, 0.28 Eo, and 0.32 Eo for the G_{zz}, G_{xx}, and G_{yy} responses, respectively. In our current implementation of the software, each of the above terrain corrections for all 4,687 stations and approximately two million triangular cells required 7 hours on a desktop PC running Windows 7 with a single

DOI http://dx.doi.org/10.1190/segam2012-0744.1

2.8 GHz processor with 8 GB RAM. This may be further optimized by increasing the discretization as a function of distance per standard practice with volume integral methods. We also note that the 3D Cauchy-type integrals are linear, and thus lend themselves to large-scale parallelization. This is the subject of our ongoing software development.

Conclusions

We have introduced the theory of Cauchy integral analogs that extend the principles of classic Cauchy integral theory to 3D potential fields. In particular, we have demonstrated how we are able to calculate the gravity and gravity gradiometry responses as surface integrals over arbitrary volumes that may have spatially variable densities. This is particularly suited to the terrain correction of AGG data that have a very large number of observation stations, have variable altitudes, and have DEMs produced from merged LiDAR and SRTM data. This method avoids prismatic discretization of the DEMs and computations associated with their volume integration as per standard practice. We have demonstrated this with a model study for a 1 Eö/√Hz AGG system from the Kauring test site in Western Australia. We note that, our ongoing research relates to implementing 3D Cauchy-type integrals for the geologically constrained 3D joint inversion of gravity and magnetic data for applications such as depth to basement and base of salt.

Acknowledgements

The authors acknowledge TechnoImaging and Rio Tinto Exploration for support of this research, and permission to publish. Zhdanov and Liu acknowledge support of the University of Utah's Consortium for Electromagnetic Modeling and Inversion (CEMI).

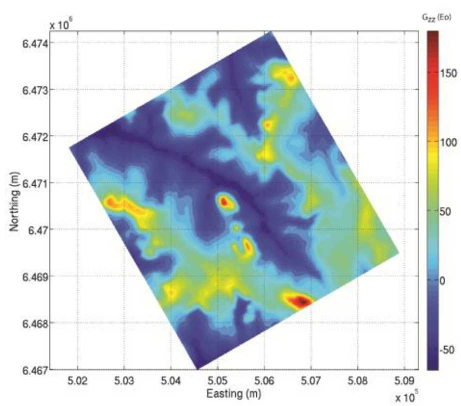

Figure 3. *Synthetic free-air G_{zz} data for the Kauring test site.*

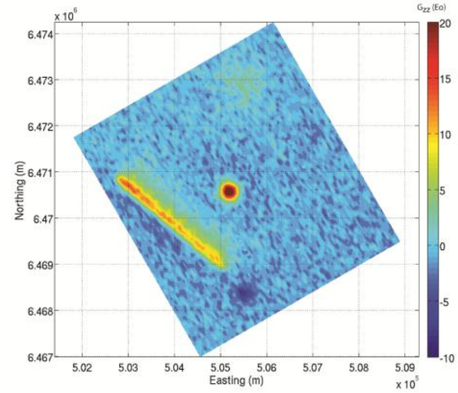

Figure 4. *Terrain corrected G_{zz} data for the Kauring test site.*

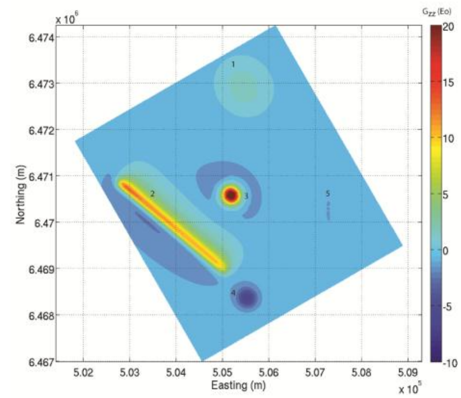

Figure 5. *Noise free terrain corrected G_{zz} data for the Kauring test site.*

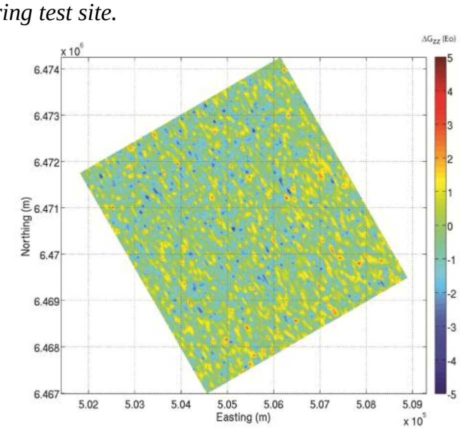

Figure 6. *The average difference between the terrain correction (Figure 4) and true model (Figure 5) is 0.34 Eö.*

© 2012 SEG

DOI http://dx.doi.org/10.1190/segam2012-0744.1

http://dx.doi.org/10.1190/segam2012-0744.1

EDITED REFERENCES

Note: This reference list is a copy-edited version of the reference list submitted by the author. Reference lists for the 2012 SEG Technical Program Expanded Abstracts have been copy edited so that references provided with the online metadata for each paper will achieve a high degree of linking to cited sources that appear on the Web.

REFERENCES

Davies, A. J., R. Foot, G. C. Joshi, and B. H. J. McKellar, 1989, Quaternionic methods in integral transforms of geophysical interest: Geophysical Journal International, **99**, 579–582.

Davis, K., M. A. Kass, and Y. Li, 2011, Rapid gravity and gravity gradiometry terrain corrections via an adaptive quadtree mesh discretization: Exploration Geophysics, **42**, 88–97.

Dransfield, M., and Y. Zeng, 2009, Airborne gravity gradiometry: Terrain corrections and elevation error: Geophysics, **74**, no. 5, I37–I42.

Grujic, M., 2012, Data processing requirements for an 1 Eö/√Hz AGG system: Presented at 22nd Conference and Exhibition, ASEG.

Howard, D., M. Grujic, and R. Lane, 2010, The Kauring airborne gravity and airborne gravity gradiometer test site, Western Australia, *in* R.J.L. Lane, ed., Airborne gravity: ASEG-PESA Airborne Gravity Workshop: Geoscience Australia Record 2010/23, 107–114.

Kass, M. A., and Y. Li, 2008, Practical aspects of terrain correction in airborne gravity gradiometry surveys: Exploration Geophysics, **39**, 198–203.

Zhdanov, M. S., 1984, Cauchy integral analogs in geophysical field theory (in Russian): Nauka.

Zhdanov, M. S., 1988, Integral transforms in geophysics: Springer-Verlag.